European Funds
Knowledge Education Development

Republic of Poland

European Union
European Social Fund

INSTYTUT METALURGII I INŻYNIERII MATERIAŁOWEJ
im. Aleksandra Krupkowskiego
Polskiej Akademii Nauk

Photovoltaic systems – theory and practice

Part 3

Marek Lipiński

Kraków 2020

Projekt nr WND-POWR.03.02.00-00-IO43/16
Międzynarodowe interdyscyplinarne studia doktoranckie z zakresu nauk o materiałach z wykładowym językiem angielskim
Program Operacyjny Wiedza Edukacja Rozwój 2014-2020, Działanie 3.2 Studia doktoranckie

Cours description

1. Introduction to photovoltaics

Basic information about the solar energy and photovoltaic Energy conversion

2. Technology of solar cells

The industrial technology of silicon solar cells and thin films solar cells will be presented

3. **Emerging photovoltaics**

Emerging materials and devices including dye-sensitized solar cell, organic solar cell, perovskite solar cell and quantum dot solar cell

4. Photovoltaic systems

Technology, applications, economics of photovoltaic systems

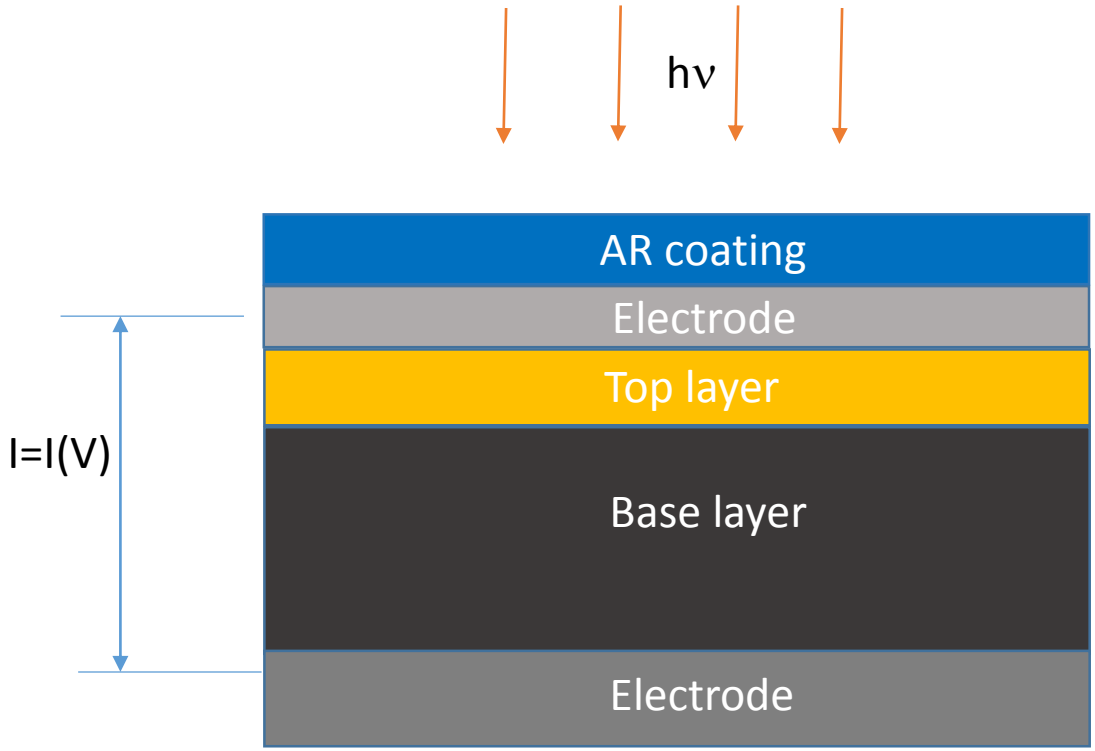

Cross sectional of a typical solar cell. The collecting electrodes are shown as the layers. The top electrode is transparent (TCO).

Photovoltaic energy conversion

The basic four steps needed for photovoltaic energy conversion:

1. Light absorption process

2. Generation a free negative - and a free positive-charge carrier pair

3. A discriminating transport mechanism, which causes the resulting free negative-charge carriers to move in one direction (to a contact that we will call the cathode) and the resulting free positive-charge carriers to move in another direction (to a contact that we will call the anode).

4. Combining with an arriving positive-charge carrier, thereby returning the absorber to the ground state.

[1]. S.J. Fonash, Solar Cell Device Physics

MATERIALS FOR SOLAR CELLS

Materials used in solar cells:

- **inorganic**
- **organic**

- **Solid :** crystalline, polycrystalline, or amorphous:
  metals, semiconductors, insulators, solide electrolytes.

type of cells: homojunction, heterojunction, metal-semiconductor, some dye-sensitized solar cells

- **Liquid materials** : electrolytes
  type of solar cells: liquid- semiconductor, dye-sensitized cells

Crystalline solids

Some Material Structure Types [1]

Material type	Size of single-crystal grain	Comments
Nanoparticle	Particle size <100 nm. single crystal, polycrystalline, or amorphous.	Spherical and columnar-like. Quantum size effects possible for particles <10 nm. Semiconductor nanoparticle when size effects are present - quantum dots
Nanocrystalline (nc) material	Single-crystal grains each < 100 nm	Polycrystalline. The nc-Si has small grains of crystalline silicon within an amorphous Si phase. Quantum size effects possible for grains <10 nm.
Microcrystalline (μc) material	Single-crystal grains <1000 μm to 100 nm.	Polycrystalline. Often simply called polycrystalline material
Multicrystalline (mc)	Single-crystal grains 1 mm.	Polycrystalline. Grains can be many cm or larger in size.
Single-crystal material	No grains nor grain boundaries.	Whole material is one crystal.

The main feature of crystalline solids: Presence of long – range order, 14 crystal lattice

[1]. S.J. Fonash, Solar Cell Device Physics

Nanoparticles and nanocrystalline solids

Higher activity

More exotic properties

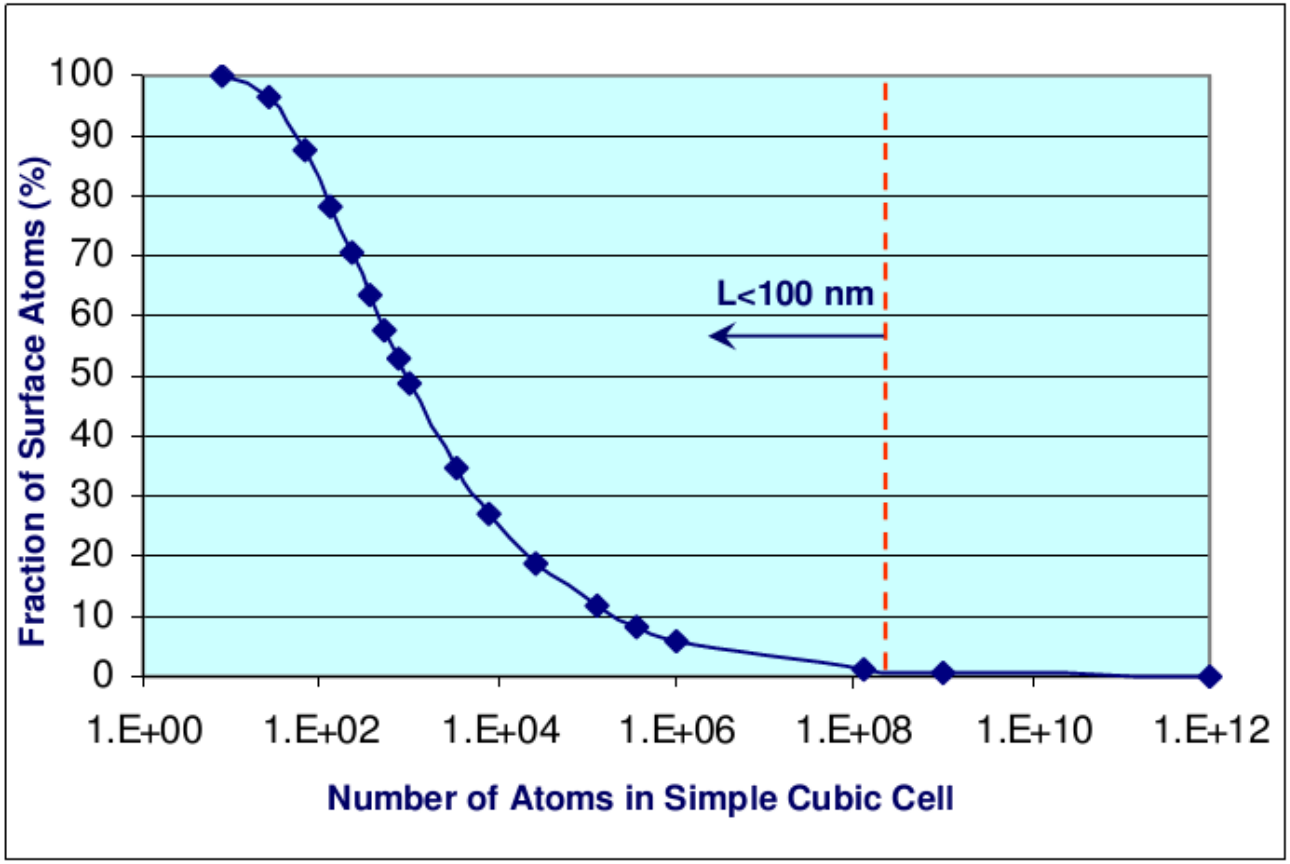

Typically, the particles smaller than 100 nm are classified as nanoparticles. When the cluster size becomes larger than 700^3 atoms (L=~100 nm), most atoms are in the bulk. Particles larger than 100 nm but smaller than optical wavelength is still of interest for optical and catalysis applications

Eal Lee, KAERI Lecture Serie, 2011

Amorphous solids

Disordered materials, contain large number of structural and bonding defects.
No long-range structural order
- there is no a unit cell and lattice

Amorphous solids are composed of atoms or molecules that display only short-range order.

Exemple: a-Si:H materials

[1]. S.J. Fonash, Solar Cell Device Physics

Crystalline solids

The 14 Bravais lattices.

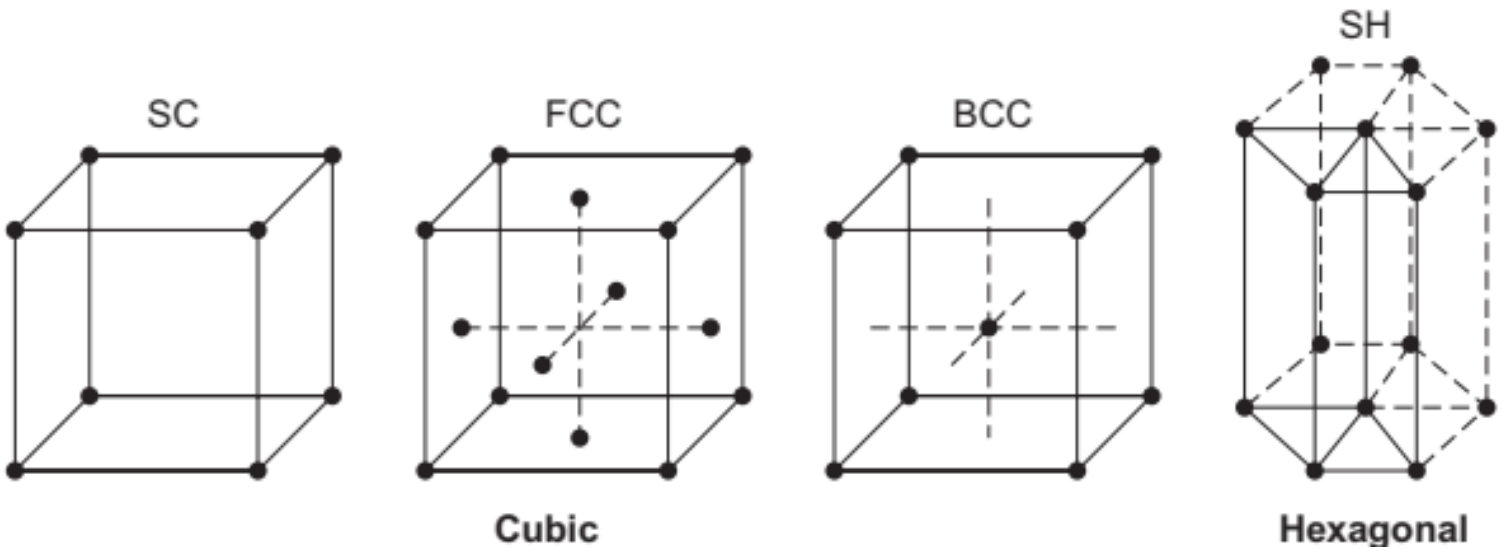

Some important unit cells: the simple cubic (SC), the face-centered cubic (FCC) the body centered cubic (BCC), the simple hexagonal (SH).

Primitive cells in reciprocal space.

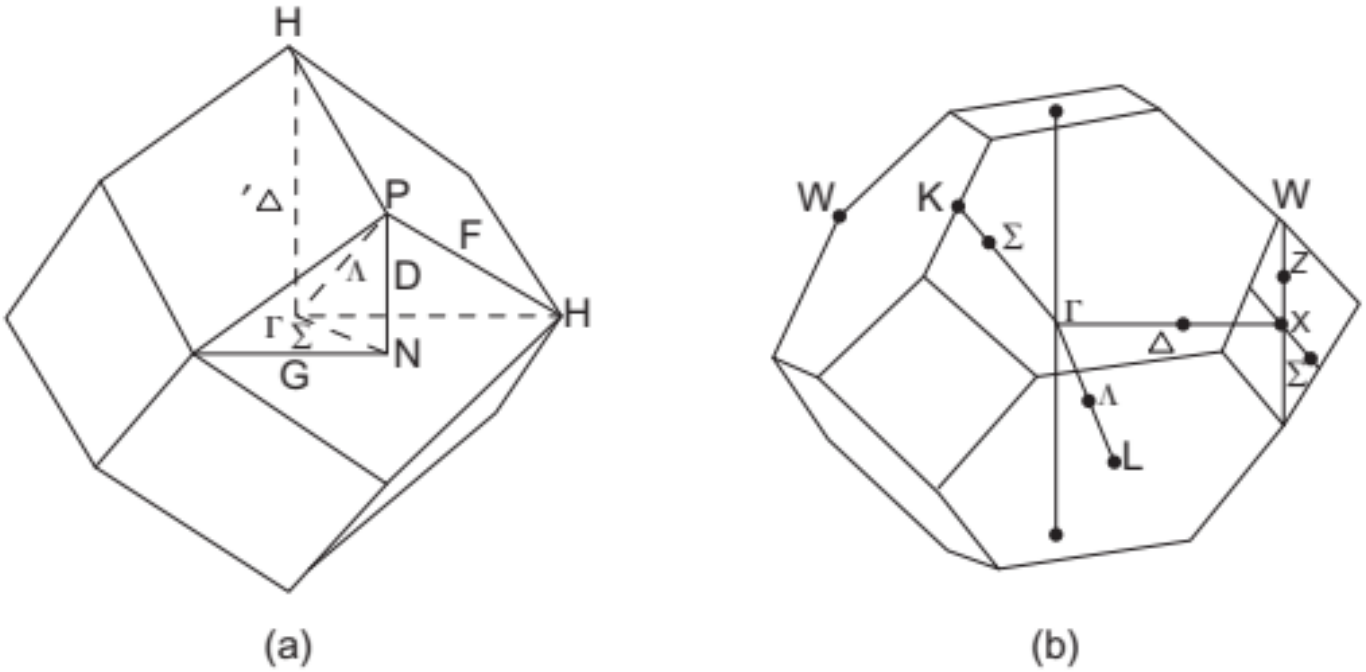

Brillouin zones for: (a) the BCC crystal lattice; (b) the FCC crystal lattice.
In the same way the Bravais lattice is divided up into Wigner –Seitz cells in the real lattice.

Phonon spectra of solids

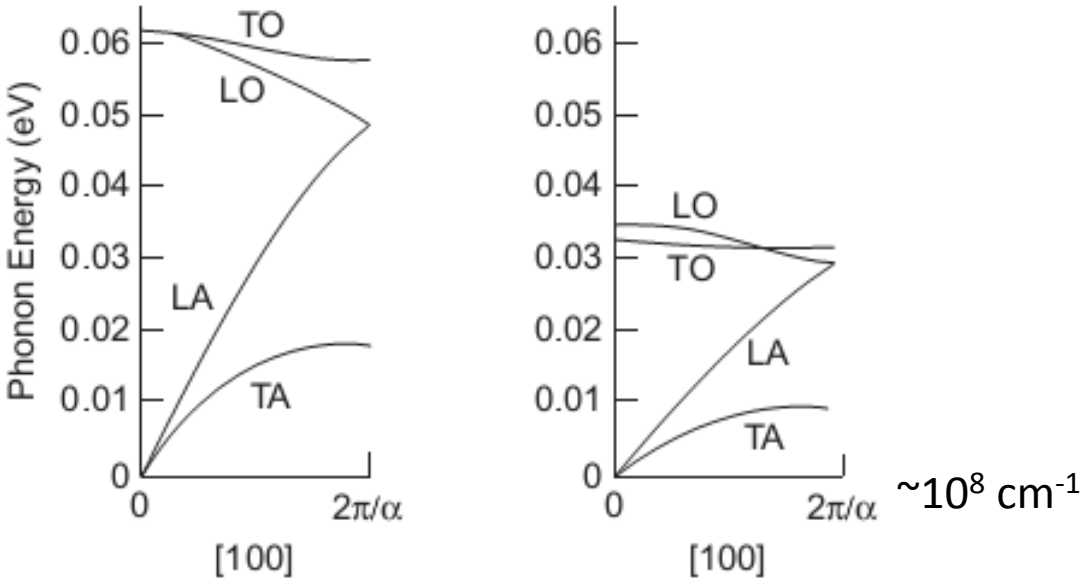

~10^8 cm^{-1}

Phonon bands in two crystalline solids: (a) silicon, and (b) gallium arsenide. Phonon bands are depicted for k values lying along the Γ to X directions in the Brillouin zone of an FCC lattice .

The momentum of the phonon for k= 2π/a (~10^8 cm^{-1}).

For comparison:
The momentum of the photons k = E_{ph}/ *h*c in the solar spectrum for E_{ph}= 1eV k ~10^6 cm^{-1}
- is very small compared to the momentum of phonons.

In single-crystal, multicrystalline, and microcrystalline materials, both total energy and total momentum are conserved in phonon – electron interactions.

For example, in a “ collision ” between an electron and phonon in a crystal (or in a crystal region in the case of polycrystalline material), the change in the k-vector of the phonon and the electron must conserve total (electron plus phonon) momentum as well as energy.

This constraint is termed the k-selection rule.

[1]. S.J. Fonash, Solar Cell Device Physics

For nanoparticle's or nanocrystalline grain's characteristic dimension approaches some multiple (5 – 50) of the lattice constant:

phonon energy corresponding to a well defined **k** -vector can disappear, also because of spatial limitations **— these changes are the result of what is termed phonon confinement.**

Heisenberg' s rule:

$\Delta x \, \Delta p \geq h \qquad \Delta x \, \Delta k \geq (2\pi)$

Δx becomes smaller due to confinement, the phonon momentum becomes ill-defined.

For small particle the vibrational modes can become discrete in energy.

Electron energy levels in solids

Single-crystal, Multicrystalline, and Microcrystalline Solids

(A) Single-electron States

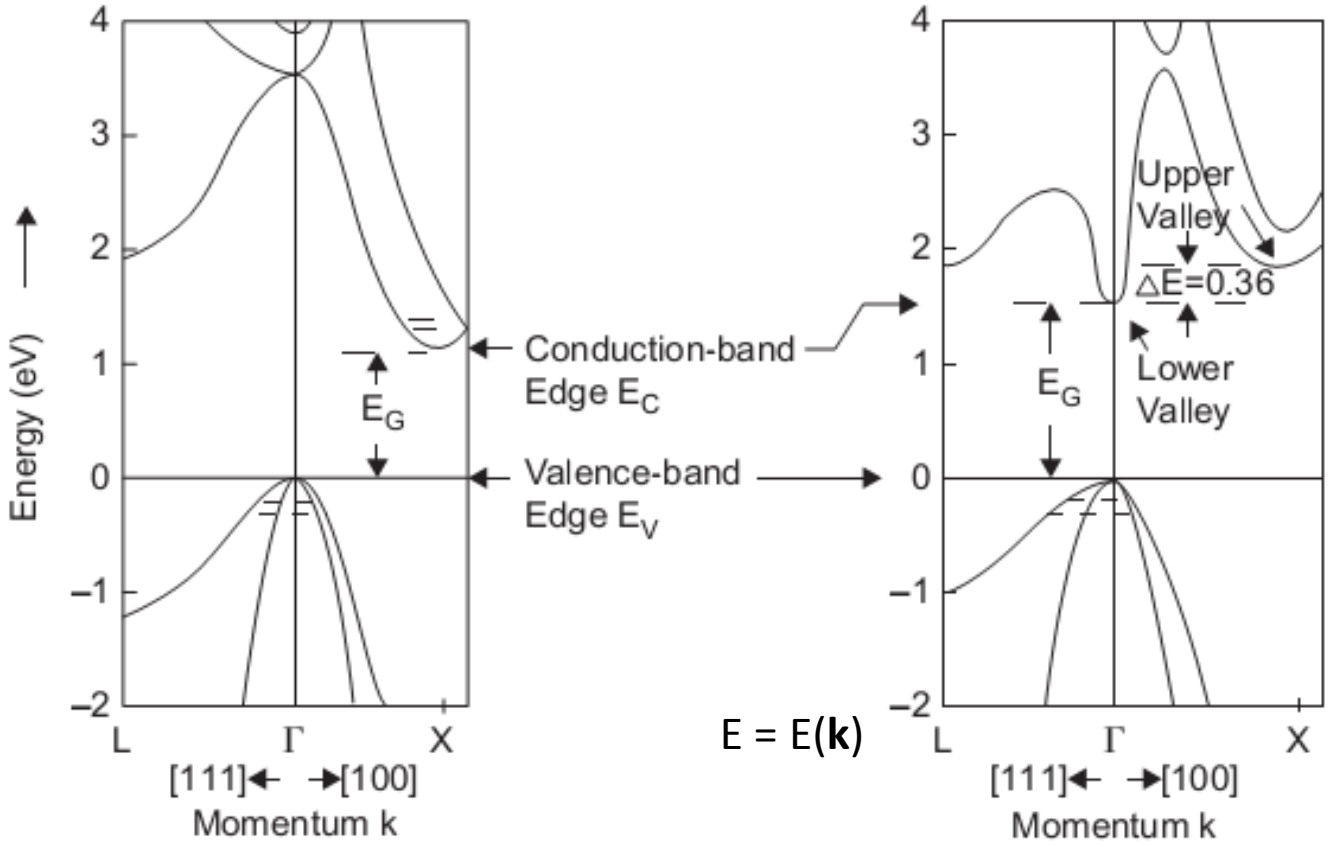

Allowed electron energies versus k-vectors (wave vectors) for two crystalline, inorganic semiconductors: (a) silicon; (b) gallium arsenide. Silicon is indirect gap (the maximum in the valence band E_V and the minimum in the conduction band E_C have different k-values); gallium arsenide is direct gap (the maximum in the valence band E_V and the minimum in the conduction band E_C have the same k-value). The valence band edges are aligned here in energy for convenience only. (After Ref. 3.)

Electron energy levels in solids

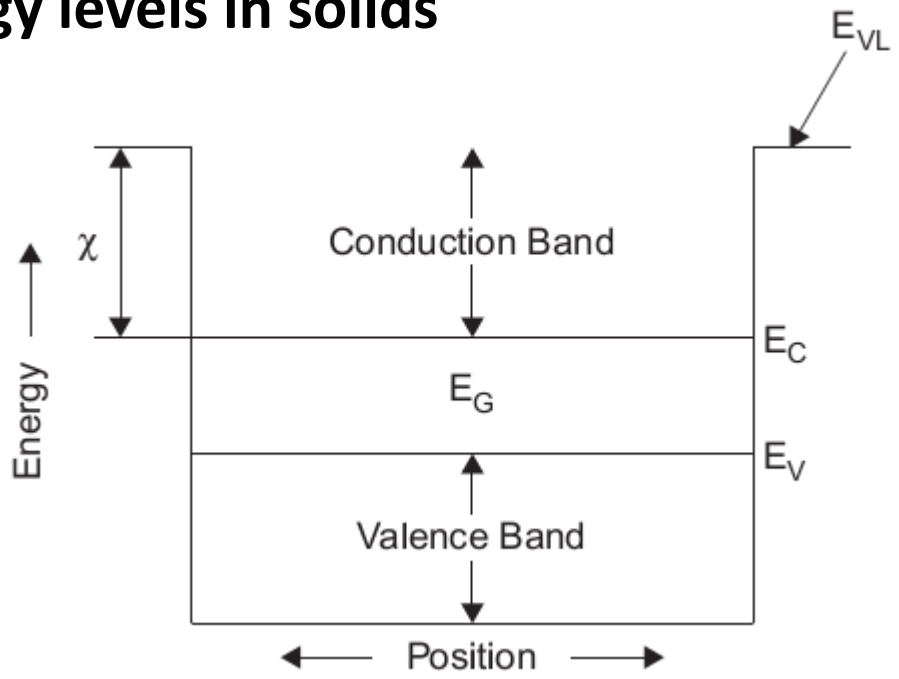

Schematic showing the energy bands available in a semiconductor as a function of position for ideal crystal. Reference energy here is the vacuum energy E_{VL}

- semiconductor $0 < E_G < 2.5$ eV
- ideal insulator $E_G \geq 2.5$ eV. The real point is that, if a material is an insulator at room temperature, then its E_G is too wide to give any significant intrinsic carrier
- metal when the gap $E_G = 0$ or when the valence electrons only partially fill the lowest band at $T = 0$.

Localized gap states found in crystalline, polycrystalline, amorphous, nanocrystalline, and nanoparticle solids may be broadly classified as acceptor-like, donor-like, or amphotericin nature. Acceptor and donor-like states are single- electron states with the following definitions.

1. **Acceptor states**. Neutral when unoccupied by an electron and, therefore, negative when occupied by an electron (ionized).
2. **Donor states.** Neutral when occupied by an electron and, therefore, positive when unoccupiedby an electron (ionized).
3. **Amphoteric gap states** can be occupied by none, one, or two valence electrons. Their charge state depends on their occupancy; e.g., one elec-tron could be the neutral state, no electrons the positively charged state, and two electrons the negatively charged situation.

It is possible to have so many gap states present in a material that they form a band within the energy gap.
These states, depending on the distance between the physical sources of the states, can be delocalized or localized in nature.
Such a band within the energy gap **is termed an intermediate band(IB).**

Excitons

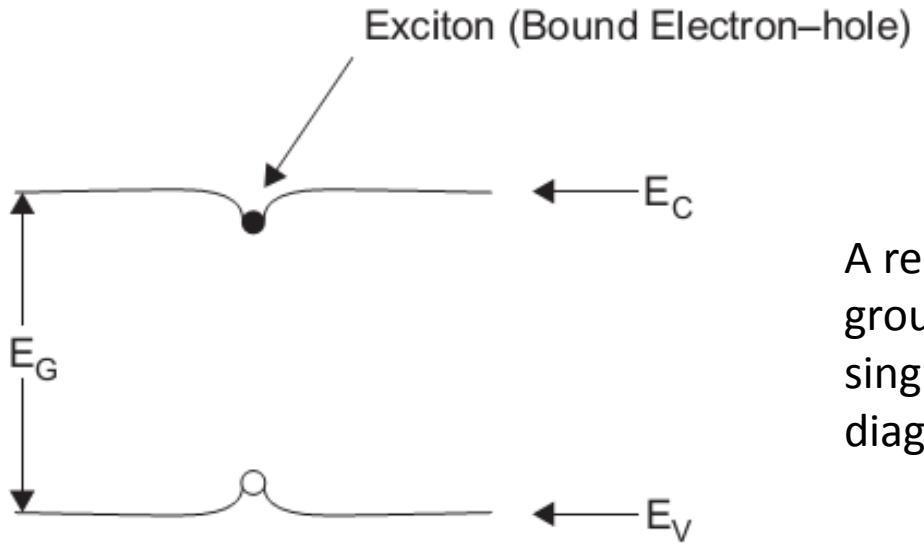

A representation of an exciton ground state superimposed on the single-electron levels of a band diagram.

Specifically, excitons are multi-electron solutions that may be viewed as an electron bound to a hole via Coulombic attraction.

The binding energy is the energy needed to have the exciton in its ground state dissociate into a free electron in the conduction band and a free hole in the valence band.

Since the binding energy is dictated by the Coulombic attraction, materials that polarize more have lower binding energies; i.e., the binding energy correlates inversely with the dielectric constant. **Excitons can be created by photon absorption and they can be mobile in a solid.**

Nanoparticles and Nanocrystalline Solids

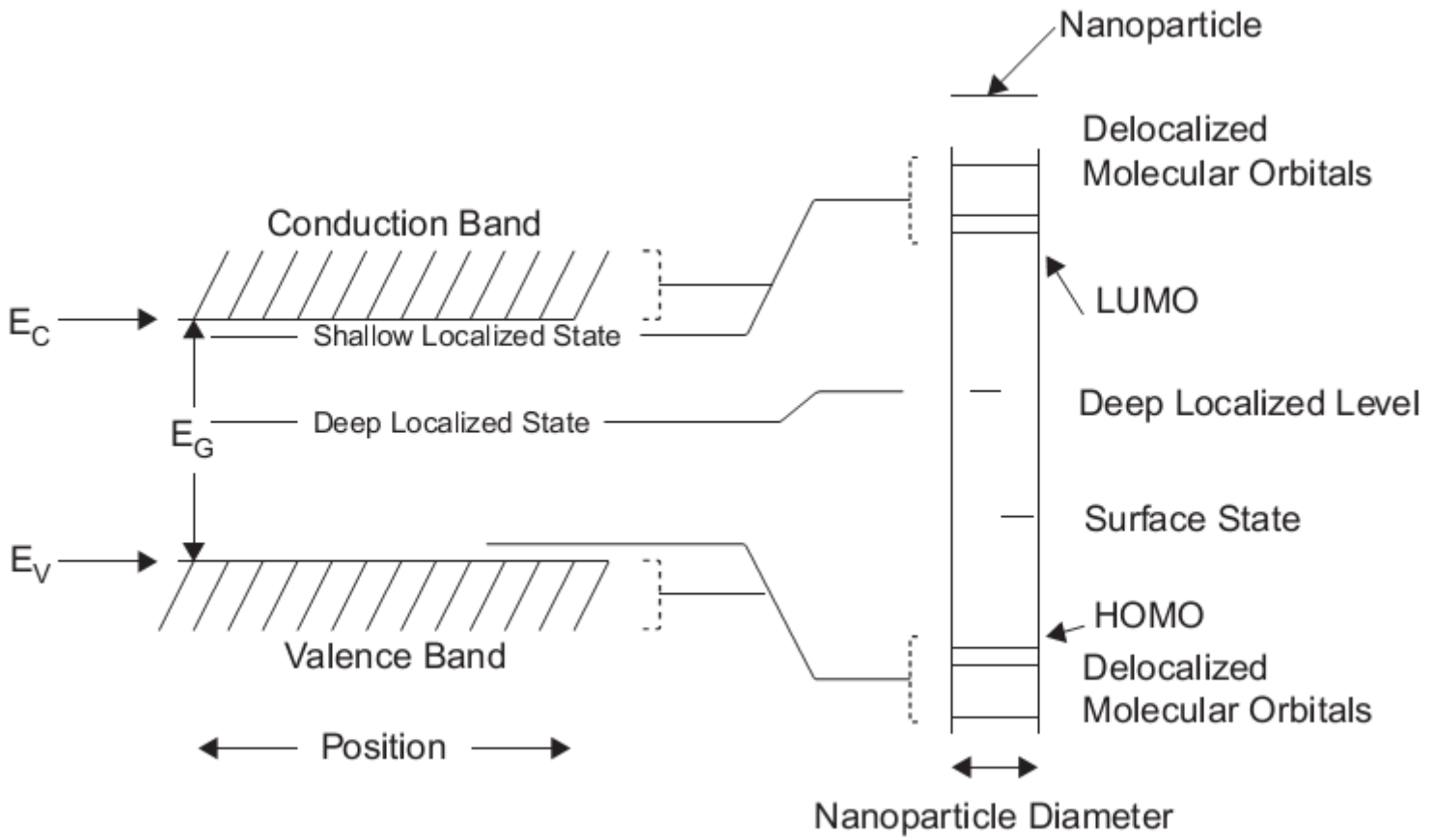

Schematic single-electron energy level diagram showing, with increasing confinement, the evolution from bands to molecular orbitals. (After Ref. 2.)

[2] A.D. Yoffe, Low-dimensional systems: quantum size effects and electronic properties of semiconductor microcrystallites (zero-dimensional systems) and some quasi-two-dimensional systems, Adv. Phys. 51 (2002) 799.

Amorphous Solids

[1]. S.J. Fonash, Solar Cell Device Physics

In amorphous solids, a vibrational mode may extend over only a few nanometers. It therefore again follows from $\Delta x\, \Delta k = \theta\, (2\, \pi)$ that phonons in disordered materials are not characterized by a well-defined wave vector **k** and **there is no phonon k - selection rule.**

The quantity k is no longer a "good quantum number."

In amorphous solids there is no Brillouin zone in reciprocal space because there is no unit cell in real space, since there is no crystal lattice. Also, in these materials, it becomes difficult to distinguish between acoustic and optical phonons.

However, in amorphous solids, phonons play the same critical roles in electron transport, heat conduction, etc., as they do in crystalline solids.

The concept of density of **k** states in reciprocal space is not valid for amorphous materials. However, the concept of a density of phonon states in energy $g_{pn}(E)$ is still valid. In fact, the $g_{pn}(E)$ of an amorphous solid will conform to that of the corresponding crystalline material to a degree depending on the importance of second nearest-neighbor, third nearest-neighbor, etc., forces.

Amorphous solids

~~E = E(k)~~

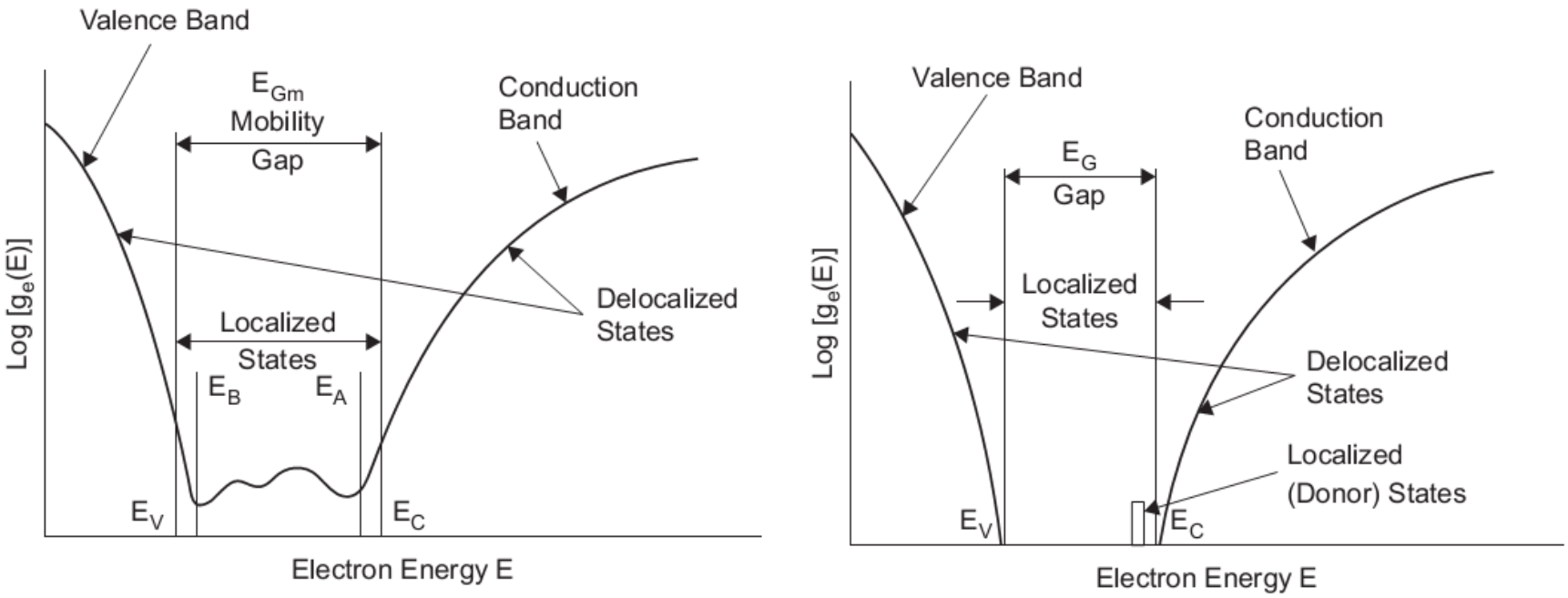

Schematic showing the density of states function $g_e(E)$ for (a) an amorphous solid and (b) a crystalline solid.

[1]. S.J. Fonash, Solar Cell Device Physics

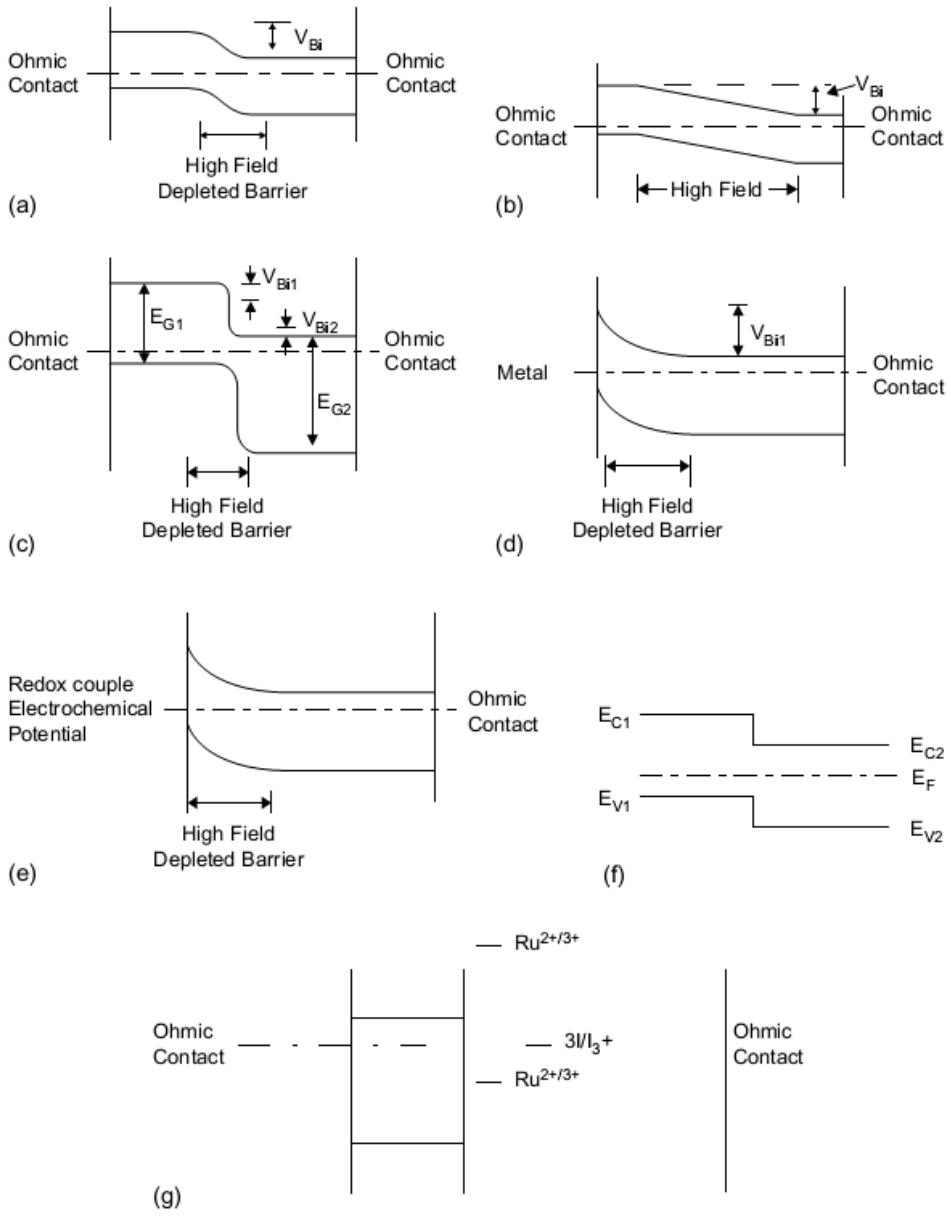

Solar cell types. Some only have a built-in electric field present as the “charge separation engine”: (a) the p–n homojunction and (b) the p- i–n homo-junction. c) the heterojunction, (d) the Schottky-barrier type cell, and (e) the semiconductor-electrolyte cell.
Some rely **solely on effective fields**: (f) a heterojunction with no built-in electric field and (g) the dye-semiconductor (shown here for the case of Ru-based dye)

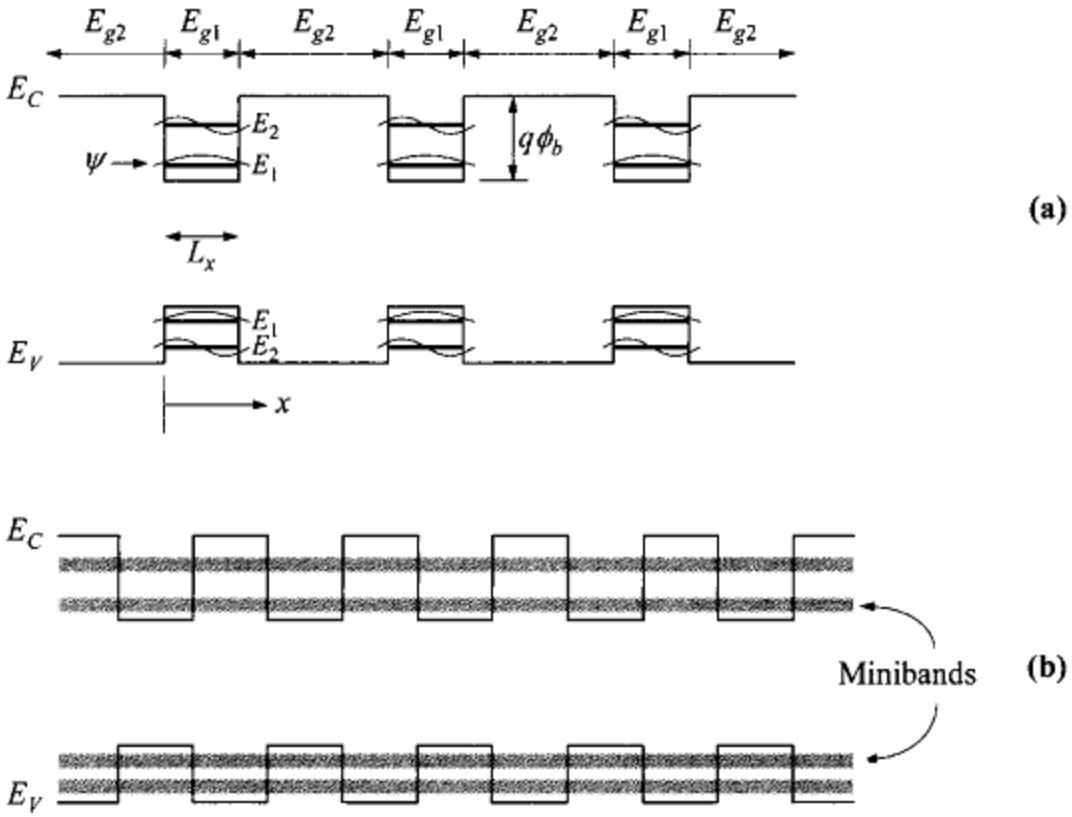

Energy-band diagrams for (a) heterostructure (composition) multiple quantum wells and (b) heterostructure superlattice

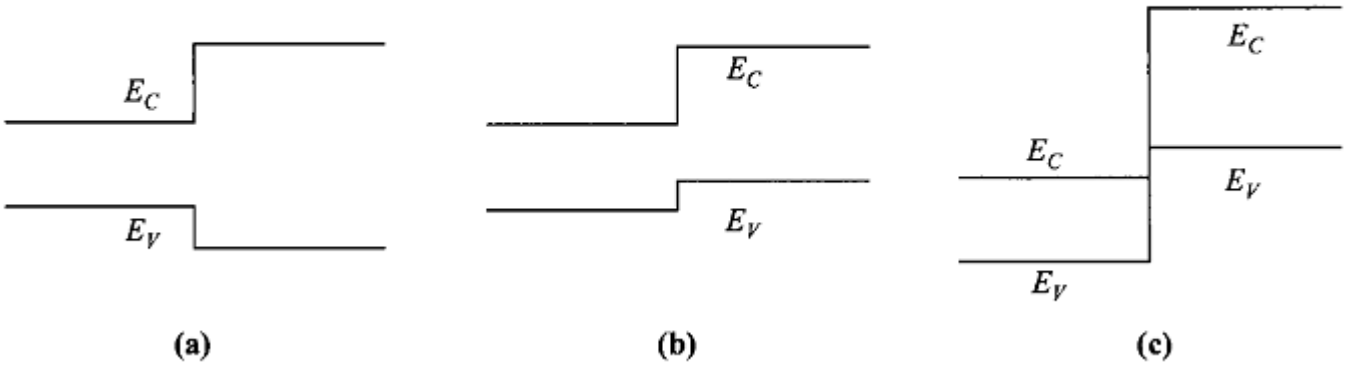

Classification of heterojunctions. (a) Type-I or straddling heterojunction. (b) Type II or staggered heterojunction. (c) Type-IIII or broken-gap heterojunction.

Absorption of light.
Light trapping.

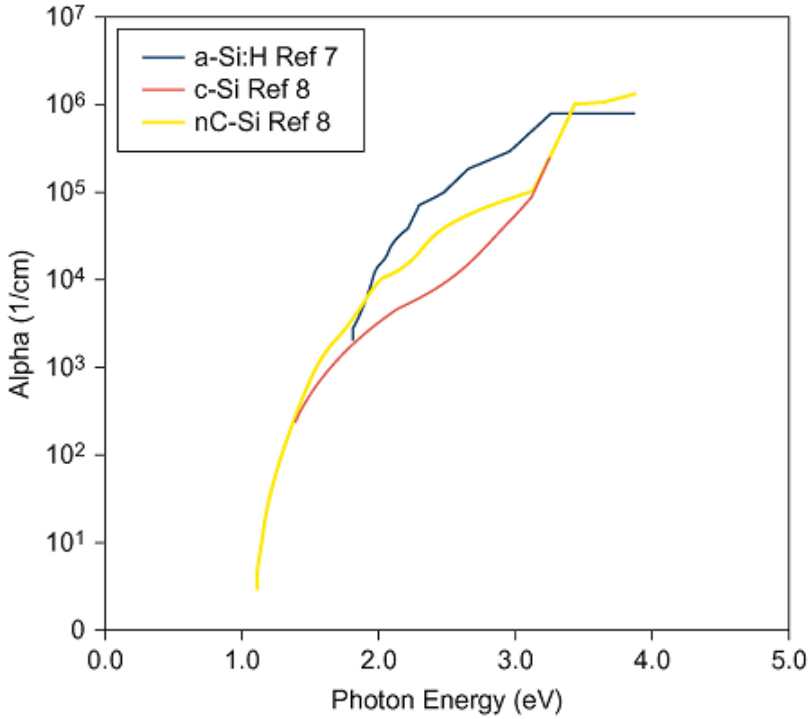

A comparison of the absorption coefficients,, for three types of silicon absorbers: an amorphous silicon-hydrogen material (a-Si:H), single-crystal silicon (c-Si), and a nanocrystalline silicon (nC-Si).

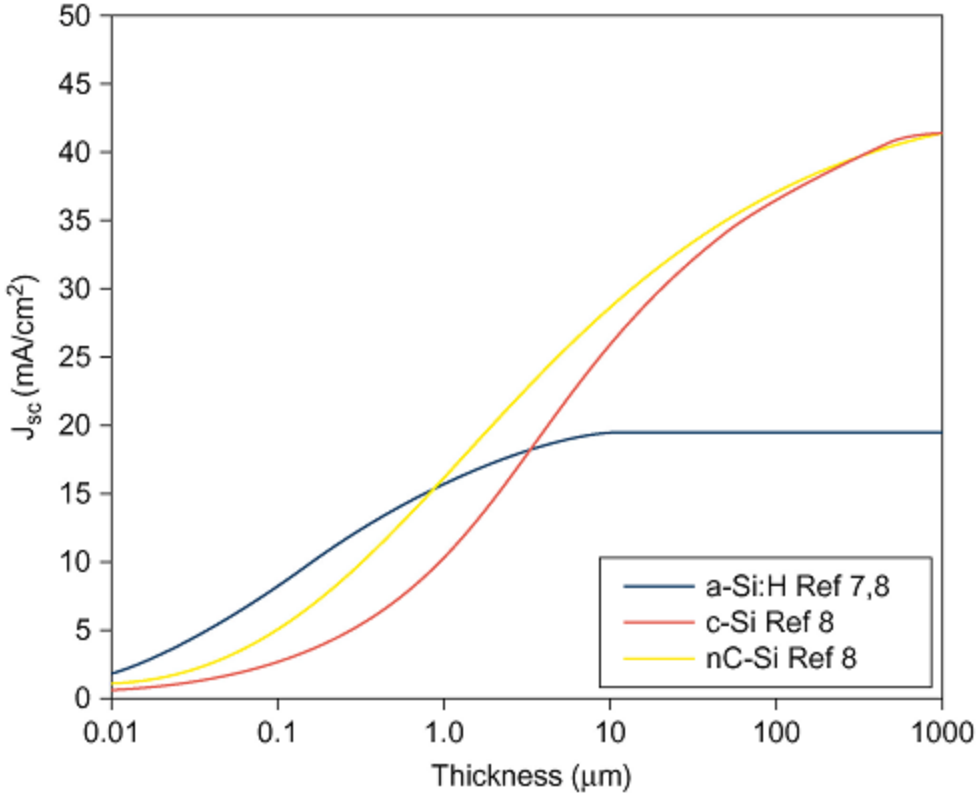

The potential J_{sc} available as a function of the log of absorber thickness for the materials, EQE = 1 is assumed.

Light trapping

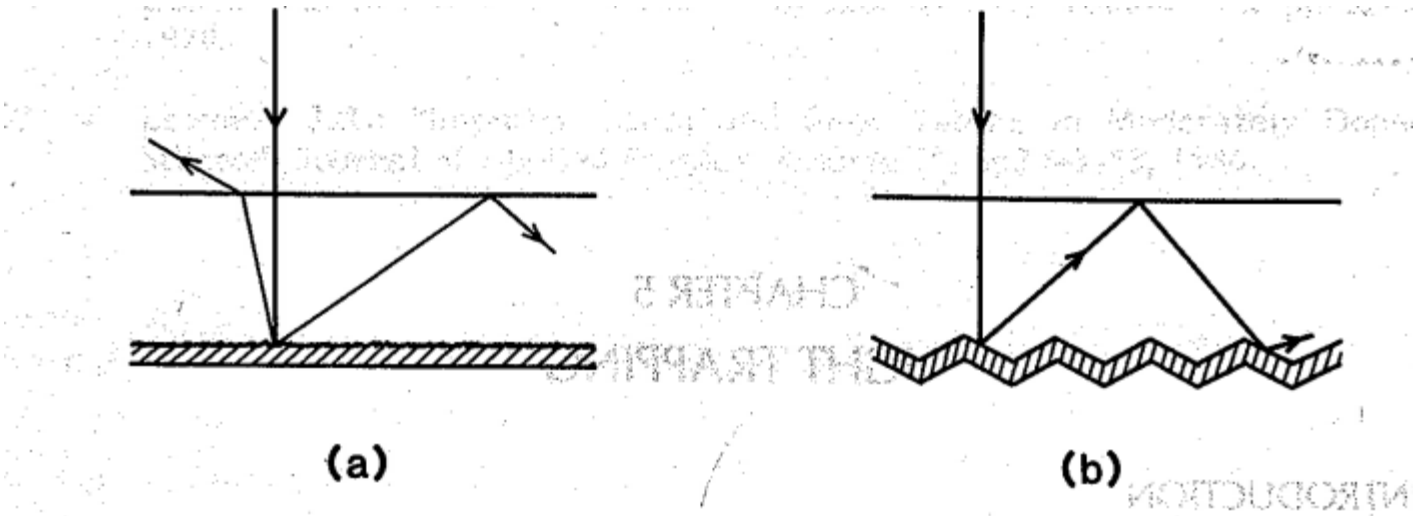

Two schemes for Trapping Light into a solar cell. (a) scheme based upon internal randomization of the light direction (Lambertian rear reflector) (b) geometrically based scheme.

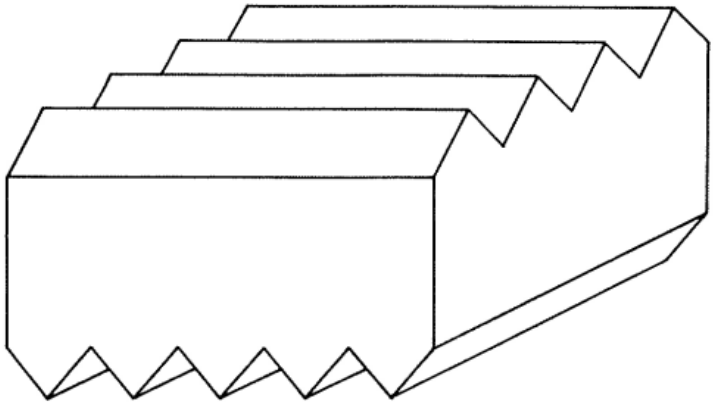

Perpendicular micro-groove scheme

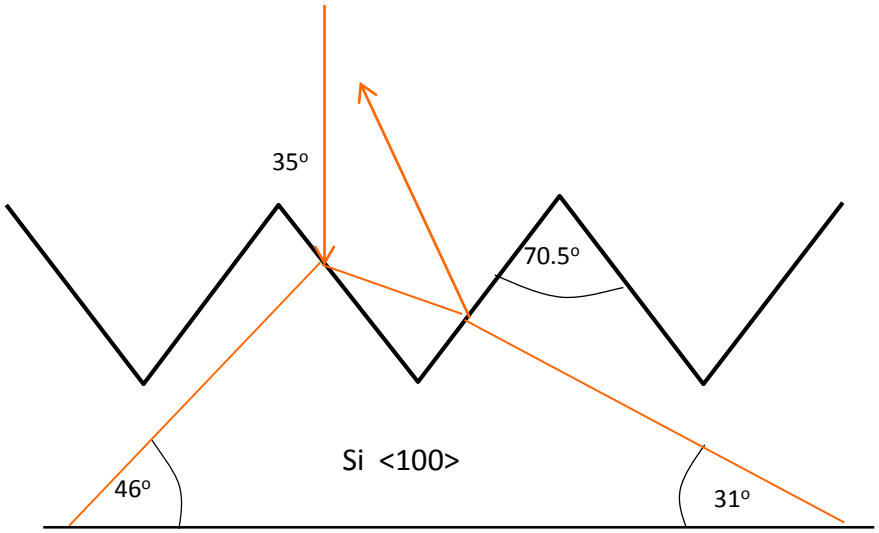

Path the light in the textured Si wafer

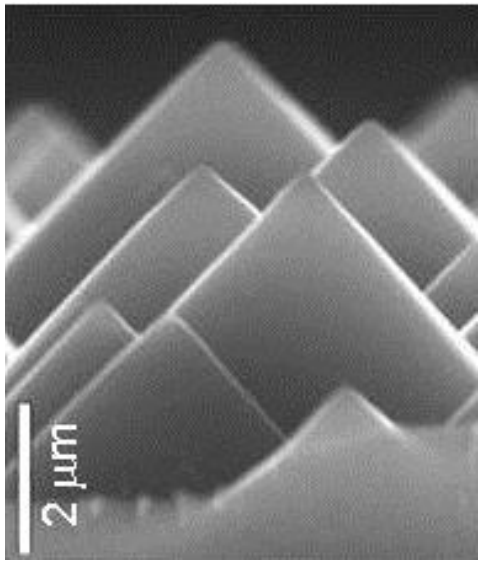

SEM of the textured surface of monocrystalline silicon (sc-Si)

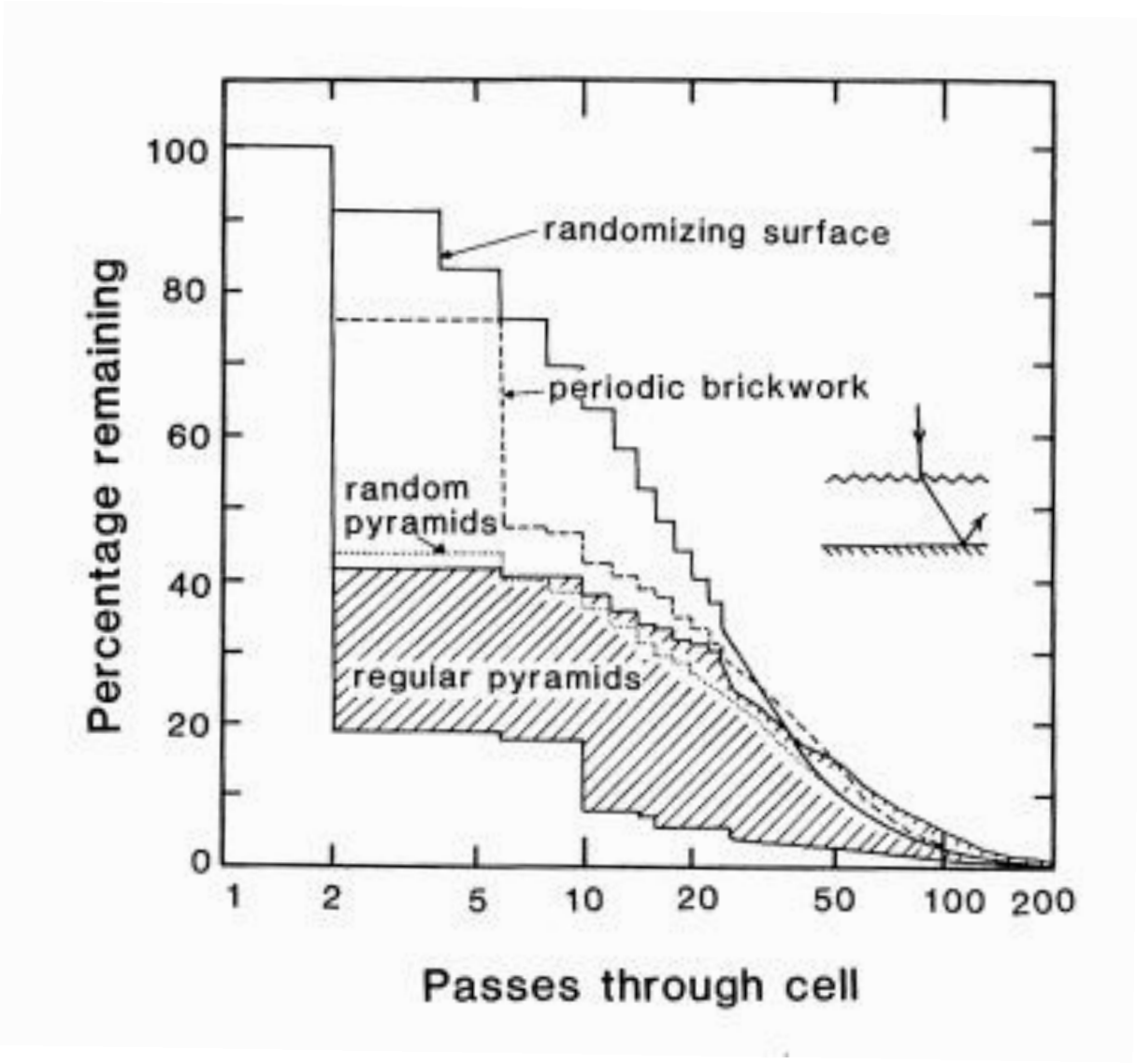
Percentage remaining
100
80
60
40
20
0
randomizing surface
periodic brickwork
random
pyramids
regular pyramids
1
2
5
10
20
50
100
200
Passes through cell

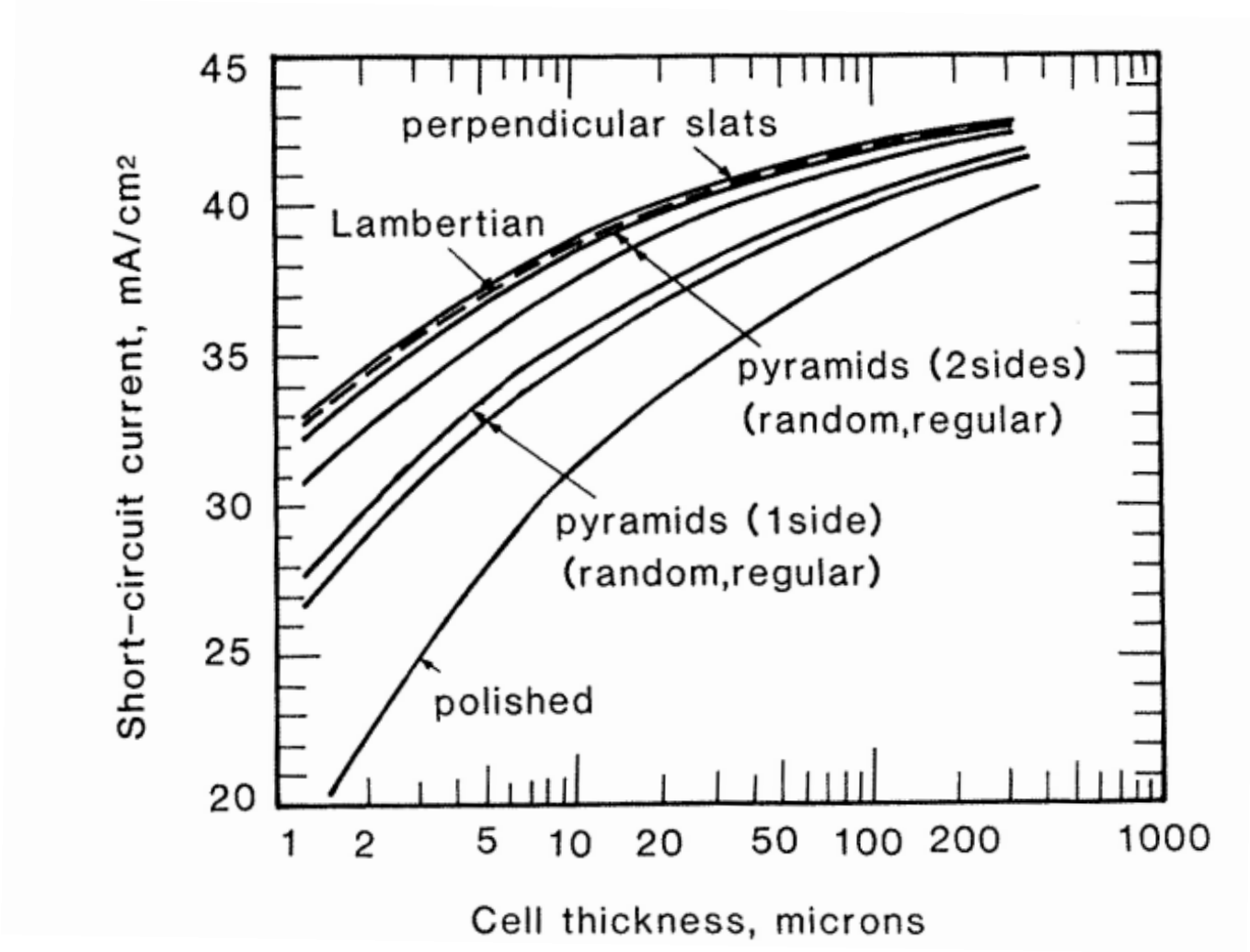
45
40
35
30
25
20
Short-circuit current, mA/cm²
perpendicular slats
Lambertian
pyramids (2sides)
(random,regular)
pyramids (1side)
(random,regular)
polished
1
2
5
10
20
50
100
200
1000
Cell thickness, microns

For thin films geometrical light trapping can not be used !

Another solution:

PLASMONIC STRUCTURES

Localized surface plasmons

Localized surface plasmons.

- Natural oscillations of the electron gas inside metal nanoparticles (e.g. gold)
- The oscillation frequency depends on the dielectric function of the metal, the environment and the shape of nanoparticles

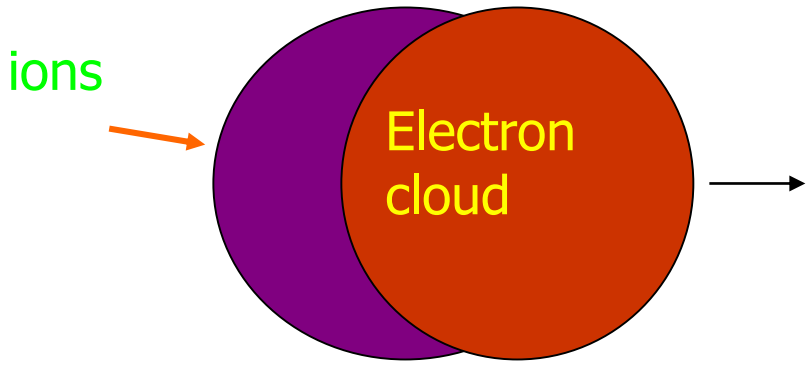

The electron cloud oscillates with the SP frequency; ions exert an electrostatic force that restores balance

Localized surface plasmons

Lycurgus Cup

IV century CE, probably made in Rome.
British Museum.

Illuminated from the inside
(transmitted light)

Localized surface plasmons

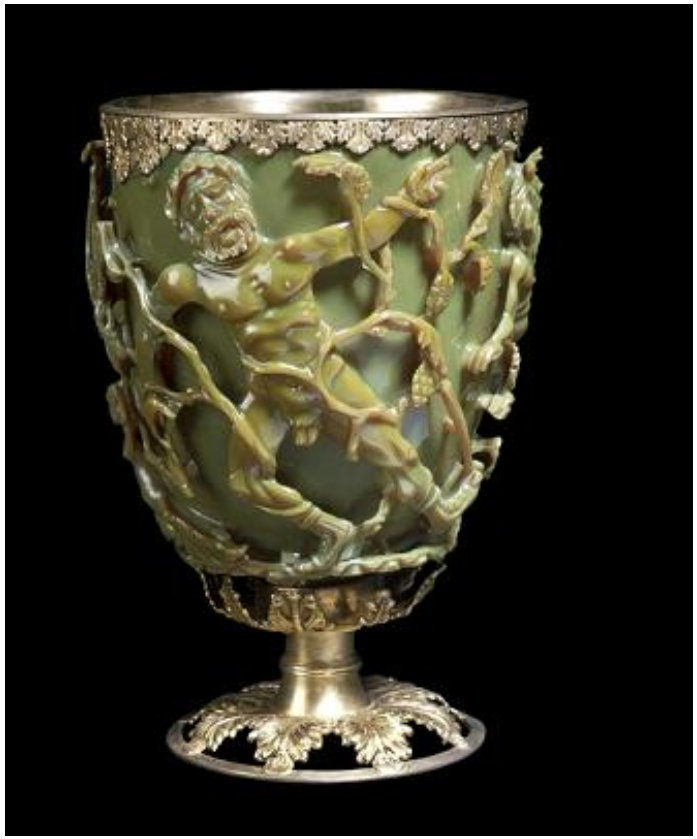

Illuminated from the outside (reflected light)

Lycurgus Cup

Localized surface plasmons

Mie theory - the exact solution of Maxwell's equations for spherical and ellipsoidal particles. For small nanoparticles R << λ quasistatic approximation. The active sections for scattering and absorption are given by the formulas:

$$C_{sct} = \frac{1}{6\pi}\left(\frac{2\pi}{\lambda}\right)^4 |\alpha|^2 \propto R^6$$

$$C_{abs} = \frac{2\pi}{\lambda} \mathrm{Im}[\alpha] \propto R^3$$

$$\alpha = 4\pi R^3 \left[\frac{\varepsilon - \varepsilon_m}{\varepsilon + 2\varepsilon_m}\right] \rightarrow$$

Resonanse: $\varepsilon = -2\varepsilon_m$

R nanoparticle radius, ε, ε_m are dielectric solid nanoparticles and medium

Definition of scattering, absorption and extinction coefficients:

$$Q_{sca} = C_{sca}/(C_{sca} + C_{abs}) \qquad Q_{abs} = C_{abs}/(C_{sca} + C_{abs})$$

$$Q_{ext} = Q_{sca} + Q_{abs}$$

For small spheres R≤40 nm: $C_{sct} << C_{abs}$ → **Heat is released, photothermal conversion**

For large spheres: (R≥100 nm): $C_{sct} >> C_{abs}$

Localized surface plasmons

(a) Influence of metal type:

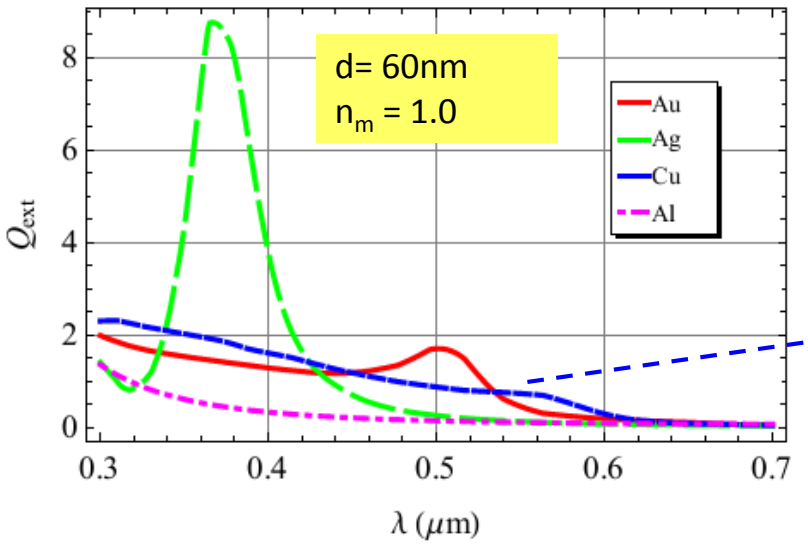

(b) Impact of the surrounding environment:

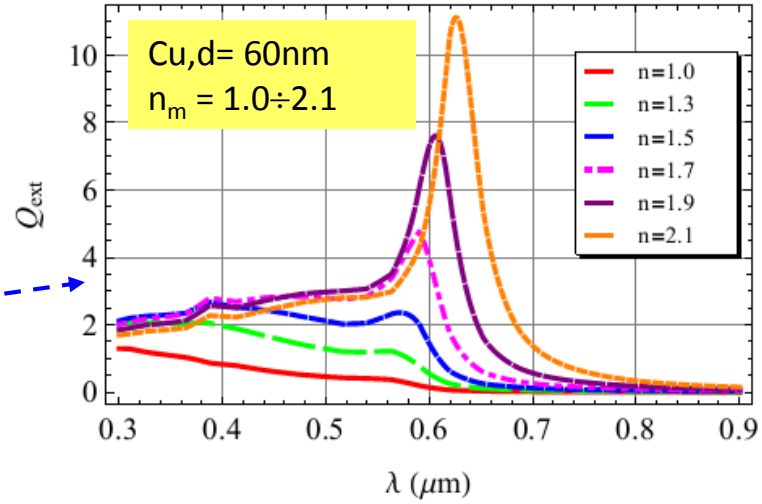

(c) The influence of diameter:

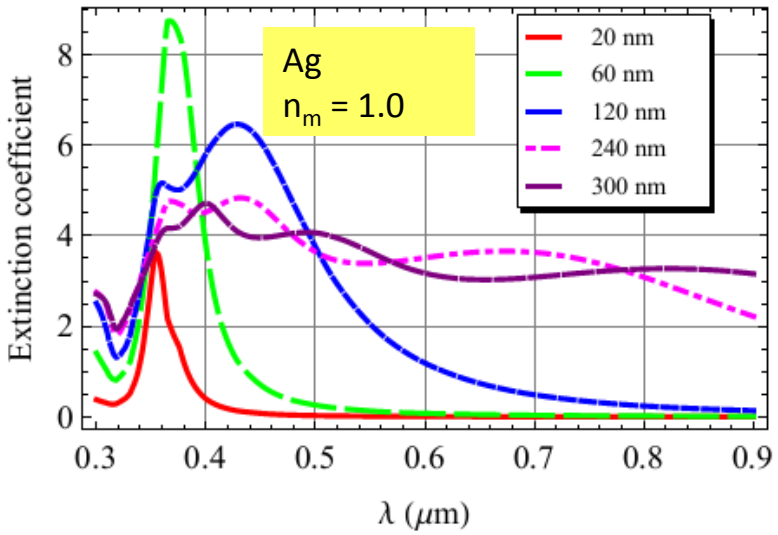

(a) Extinction coefficient (d=60nm, n_m=1)

(b) ncrease of refractive index:
- resonance shift towards longer waves
- narrowing of the resonance peak,
- amplitude increase

(c) dipole resonance, for d> 60 nm multipole resonance

Sarid D. and. Challenger W, *Modern Introduction to Surface Plasmons*, Cambridge Univ.Press, 2010

Localized surface plasmons

Near field Simulations – theory Mie [Sarid,2010]

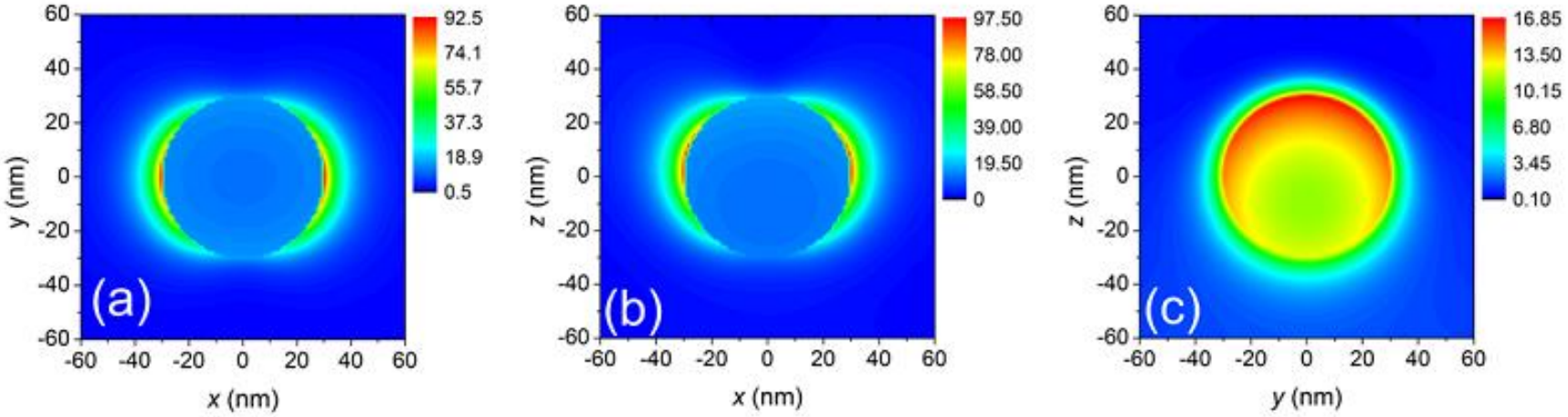

Field strength, IEI^2, surrounded by a spherical silver particle d = 60 nm in the air for a resonant wavelength of 367 nm, for a flat wave running in the z-axis and polarized in the x-axis. Simulation - Mie theory.

Strengthening the field strength over 10 times!

[Sarid,2010] D. Sarid and W. Challenger, Modern Introduction to Surface Plasmons, Cambridge Univ..Press, 2010, str.202.

Applications

- Chemical and biological sensors (used commercially)
- Medical diagnosis and procedures using Au spherical particles and nanoshells (in commercialization), nanomedicine, teranostics (teradiagnostics)
- *Other, not yet commercial:*
- Nanophotonic applications
- SERS (Surface-Enhanced Raman Spectroscopy)
- Heat-assisted magnetic recording
- Metamaterials
- Super lenses, optical invisibility
- **Photovoltaics**

Localized surface plasmons for solar cells. Light trapping.

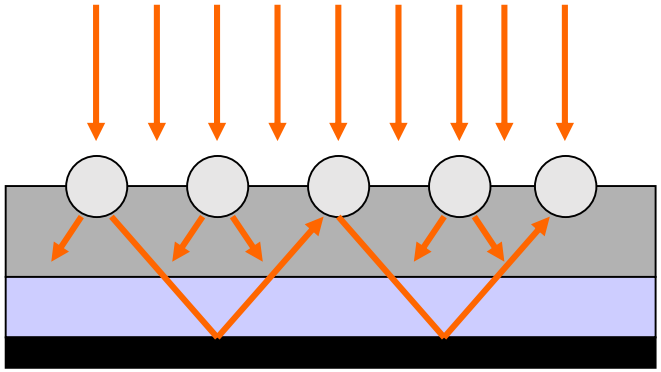

Scattering by metal particles on the cell surface. The optical path extension of light in a semiconductor.

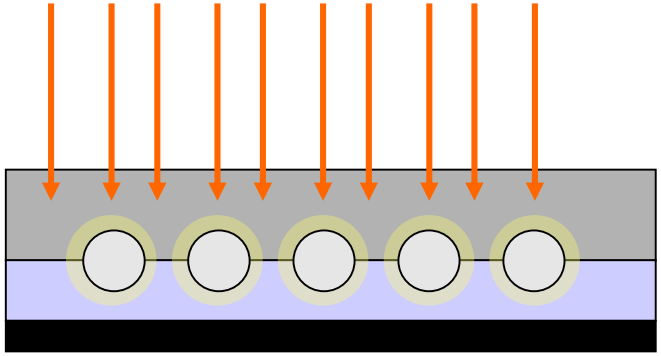

Excitation of localized surface plasmons by metal particles immersed in a semiconductor. The near field of excited particles generates charge carriers

The absorber thickness can be reduced 10-100 times without affecting the efficiency of the cell !

H. A. Atwater and A. Polman, *Plasmonics for improved photovoltaic devices*, Nature materials, 9(2010)205-213

Three generations of solar cells. Limits of efficiency

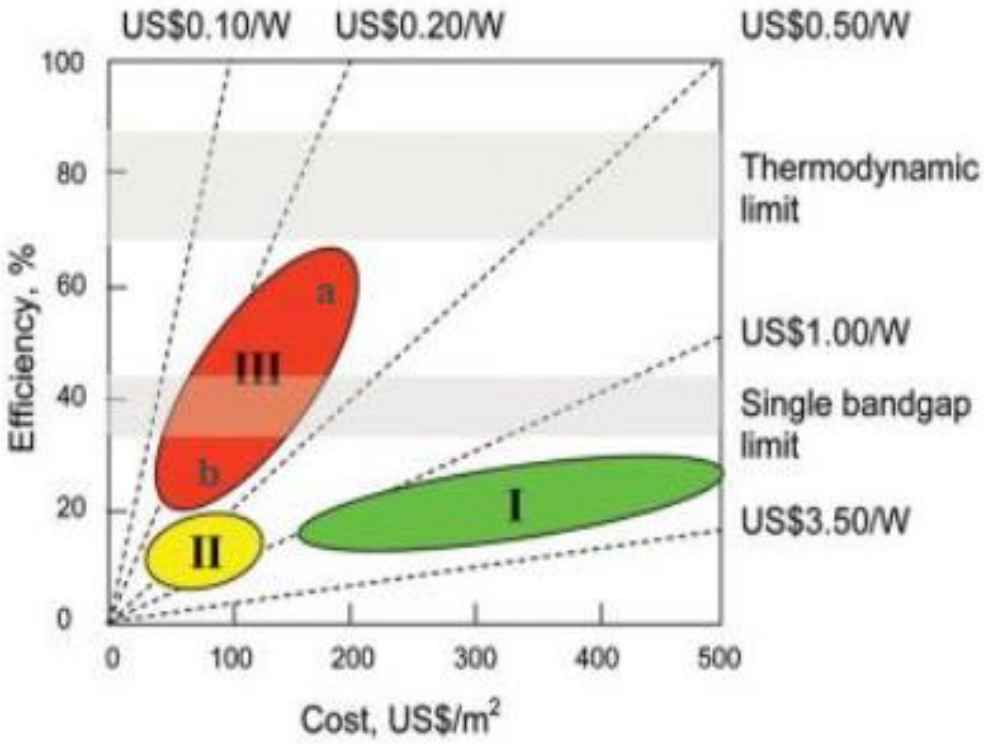

Region IIIa depicts very high-efficiency devices that require novel mechanisms of device operation.

Region IIIb depicts the region in which organic PV devices with moderate efficiencies and very low costs.

Average exchange conversion factor for the year 2012: 1US$=0.76 €.

Figure 3: Cost-efficiency analysis for 1st, 2nd and 3rd generation PV technologies (I, II, and III, respectively)

[Adapted from M. Green "Third Generation Photovoltaics", Springer-Verlag, 2003]

JOURNAL OF APPLIED PHYSICS VOLUME 32, NUMBER 3 MARCH, 1961

Detailed Balance Limit of Efficiency of *p-n* Junction Solar Cells*

WILLIAM SHOCKLEY AND HANS J. QUEISSER
Shockley Transistor, Unit of Clevite Transistor, Palo Alto, California
(Received May 3, 1960; in final form October 31, 1960)

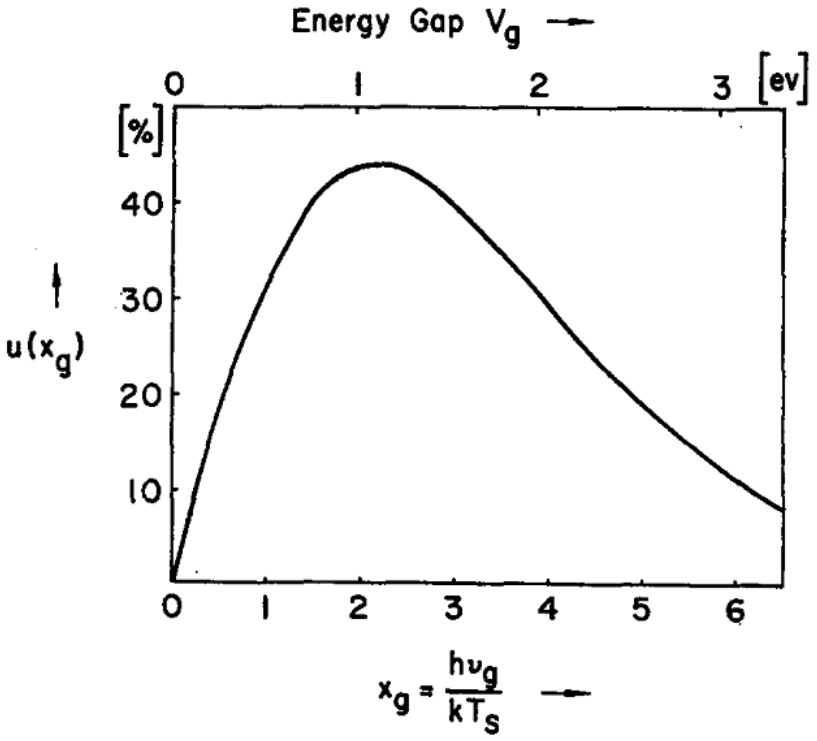

For black body radiation (6000 °C) and maximum concentration

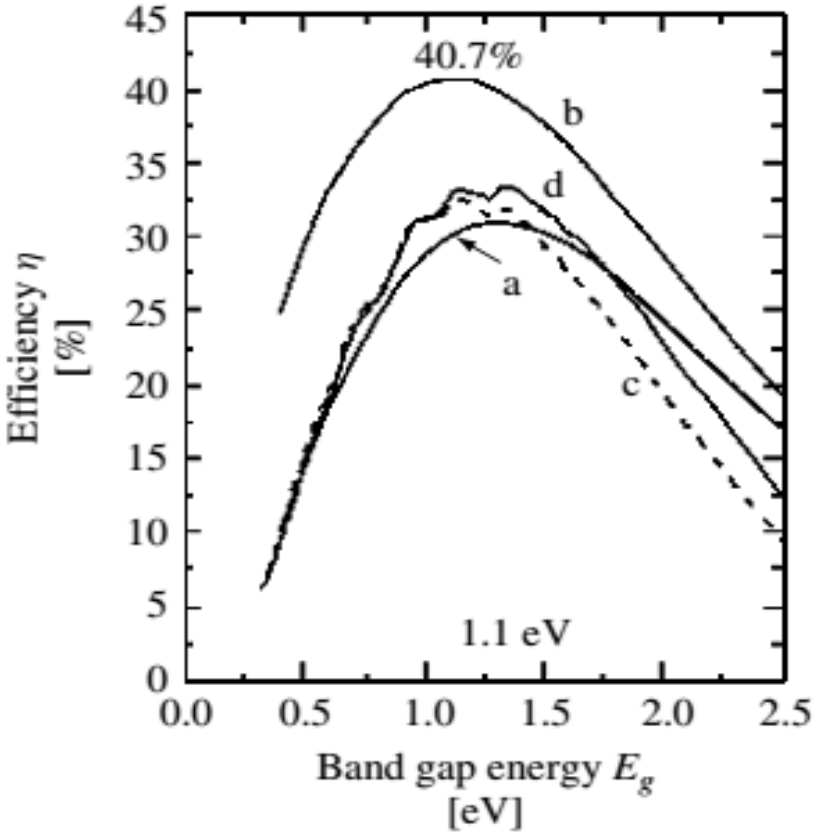

SQ efficiency limit for an ideal link for unconcentrated radiation of a perfectly black body, highly concentrated and for the Earth's solar spectrum: (a) non-concentrated radiation of a perfectly black body 6000 K (1595.9 Wm^{-2}); b) fully concentrated 6000 K (7349.0 x 10^4 Wm^{-2}). C) unconcentrated AM1.5-direct (767.2 Wm^{-2} and d) AM1.5 Global (962.5 Wm^{-2})

Handbook of Photovoltaic Science and Engineering, Ed: A. Luque and S. Hegedus , J. Wiley, 2003, p.123.

- **In thermal equilibrium: the absorption of each photon is balanced by the emission of the photon.**
- **The spectrum of radiation in a semiconductor in conditions of thermal imbalance - Planc's generalized law introduced by Würfel:**

$$n_{abs}\left(E_g, T_s, \Omega_{abs}\right) = \frac{2\Omega_{abs}}{c^2 h^3} \int_{E_g}^{\infty} \frac{E^2}{\exp\left(\frac{E}{kT_S} - 1\right)} d(E)$$

$$n_{emit}\left(E_g, T_c, \Omega_{emit}\right) = \frac{2\Omega_{emit}}{c^2 h^3} \int_{E_g}^{\infty} \frac{E^2}{\exp\left(\frac{E-qV}{kT_c} - 1\right)} d(E)$$

$\frac{\Omega_{emit}}{\Omega_{abs}} = 1$ or maximum light concentration f_{max} :

$\boldsymbol{f_{max} = (d_{zs}/r_s)^2 = 46\,198\,(2)}$ **for vaccum**

where :

d_{zs} the distance from the Earth to the Sun, and r_s the radius of the Sun.

$\mu = qV$ electrochemical potential, Gibbs free energy

maximum light concentration f_{max} for medium of refractive index *n:*

$$f_{max} = (d_{zs}/r_s)^2 \, n^2$$

Concentrators approaching this limiting performance actually have been built. The present record concentration ratio of 84,000 an output power of 7.2 kW/cm^2

M. Green, *Third Generation Photovoltaics*, Advanced Solar Energy Conversion, Springer, 2003.

Smestad G, Ries H, Winston R and Yablonovitch E (1990), The thermodynamic limits of light concentrators, Sol En Matls 21: 99-111

$$J = qn_{abs} - qn_{emit}$$

$$J_{max} = q(n_{abs} - n_{emit}(V_{max}))$$

$$qV_{max} \approx E_g\left(1 - \frac{T_c}{T_s}\right) - kT_c \ln\left(\frac{\Omega_{emit}}{\Omega_{abs}}\right)$$

$$I = I_{ph} - I_0\left[\exp\left(\frac{V}{V_t}\right) - 1\right]$$

Hirst L.C., Ekins-Daukes N.J., *Fundamental losses in solar cells*, Prog. Photovolt. Res. Appl. 2011, 19, 286–293.

Fundamental losses in the 1st and 2nd generation cells.

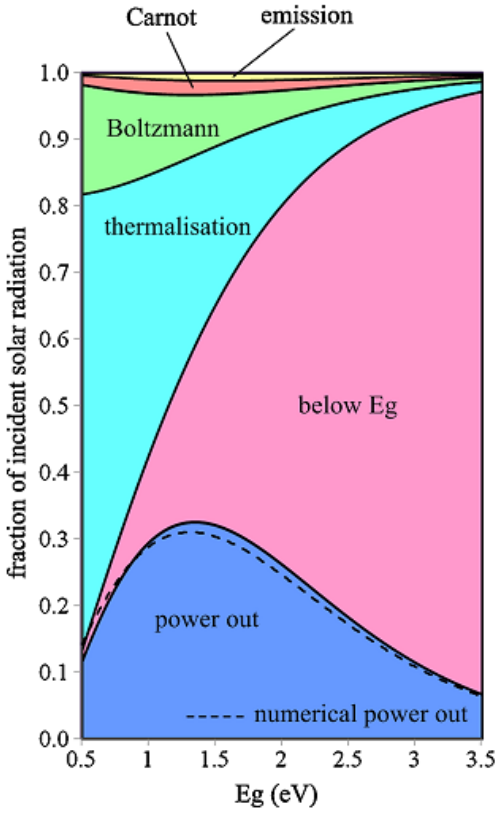

Mechanisms of power losses in the cell depending on Eg (Hirst, 2011).

Hirst L.C., Ekins-Daukes N.J., *Fundamental losses in solar cells*, Prog. Photovolt. Res. Appl. 2011, 19, 286–293.

Fundamental losses in the 1st and 2nd generation cells.

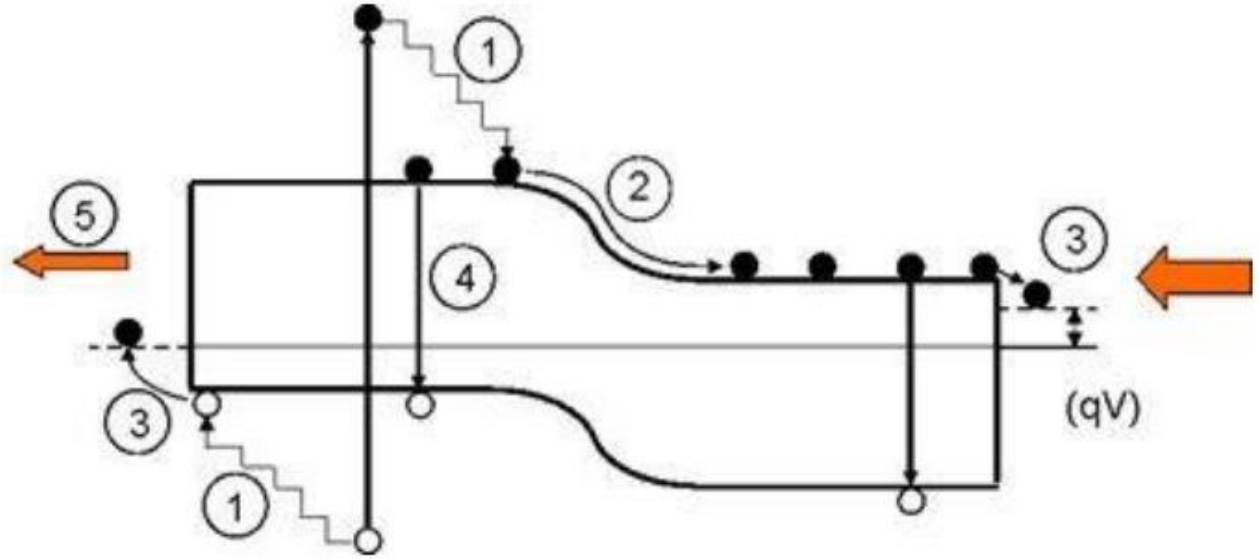

Energy losses in a single-junction solar cell:

(1) **Thermalization of Eph > Eg carriers (losses ~ 47%)**

(2) Voltage loss at the junction

(3) Voltage loss on contacts

(4**) Recombination radiant (~ 1.5%)**

(5) **No absorption of E_{ph} <E_g photons (1.12 eV for Si) (losses ~ 18.5%)**

M.A. Green, *Physica* E **14 (**2002) 11, M. C. Beard i wsp., *Nano Letters*, 7(2007) 2506

Landsberg Limit

$$\dot{E}_S = \dot{W} + \dot{Q} + \dot{E}_C$$

$$\dot{S}_S = \dot{S}_C + \dot{S}_A$$

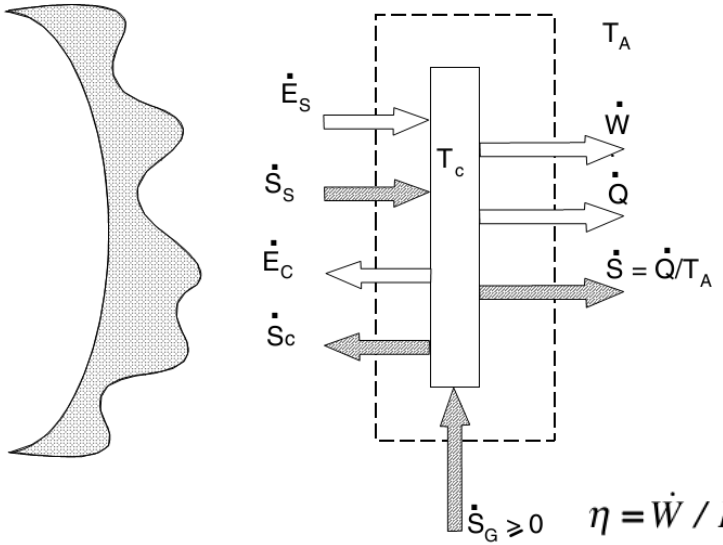

$$\dot{E}_S = \sigma T_S^4$$

$$\dot{E}_C = \sigma T_C^4$$

$$\dot{S}_S = \frac{4}{3}\sigma T_S^4$$

$\dot{S}_G$ entropy generation flux

$$\eta = \dot{W} / \dot{E}_S = (1 - \frac{4}{3} T_A / T_S) - T_C{}^4 (1 - \frac{4}{3} T_A / T_C) / T_S{}^4 - T_A \dot{S}_G / \dot{E}_S$$

For $S_G = 0$ maximum for $T_C = T_A$ which give the Landsberg limit:

$$\eta_L = 1 - \frac{4}{3} T_A / T_S + \frac{1}{3} T_A{}^4 / T_S{}^4$$

η = 93.3 %

M. Green, *Third Generation Photovoltaics*, Advanced Solar Energy Conversion, Springer, 2003.

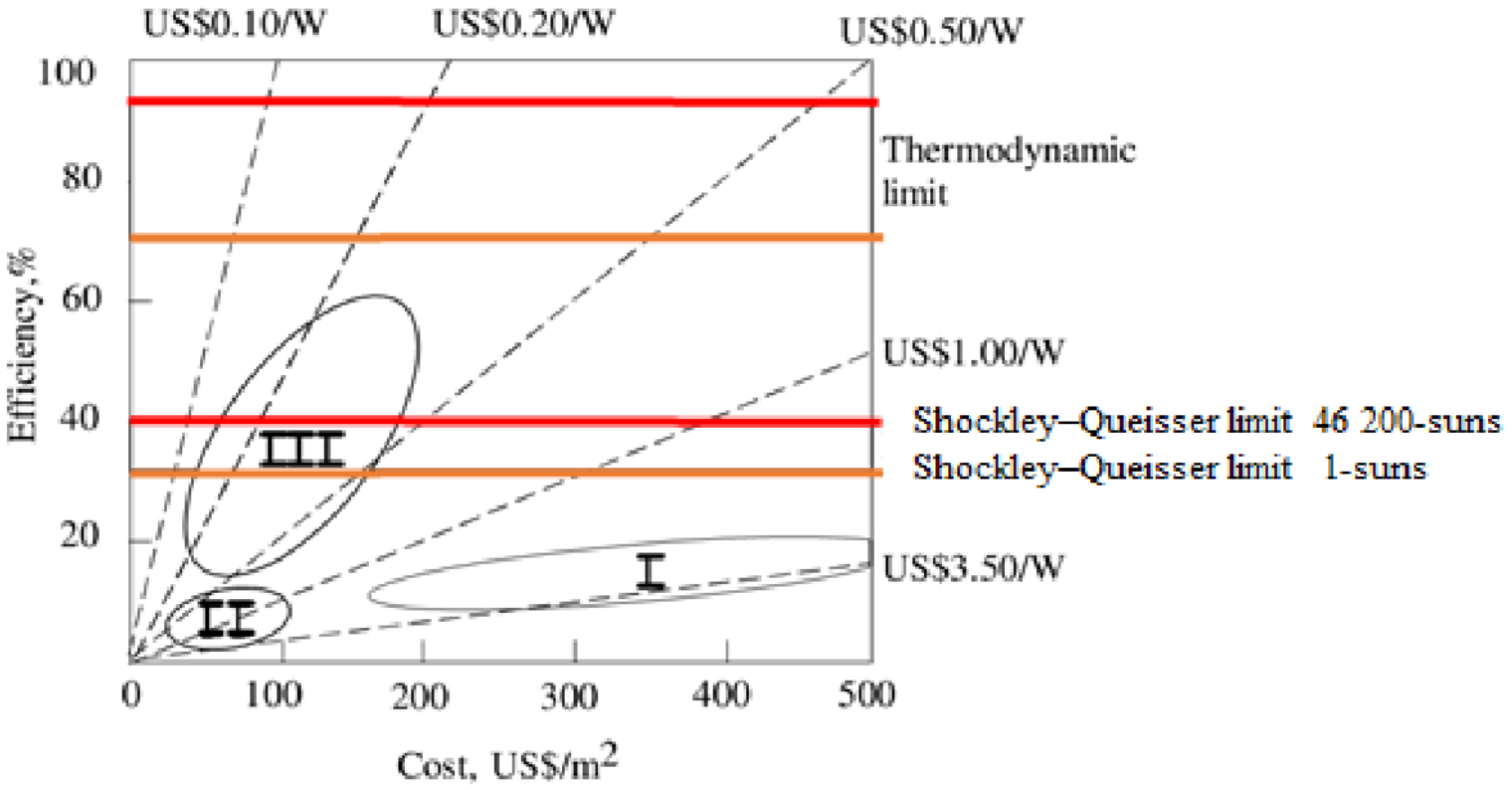

GREEN M.A., *Third generation photovoltaics: advanced solar electricity conversion*, Springer-Verlag, Berlin Heidelberg, 2006

Third generataion solar cell –
very high efficiency (region 3a)

Third generataion solar cell - very high efficiency (region 3a)

	Spectral conversion	Spectral splitting	Using excess energy
1 photon ↓ 1 electron		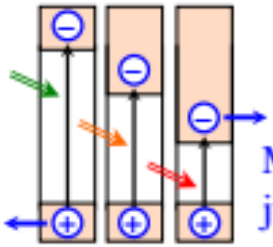 Multi-junction	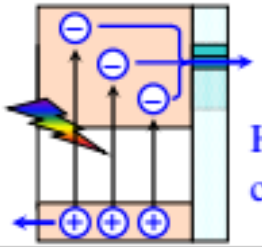 Hot-carrier
2 particles (low energy) ↓ 1 particle (high energy)	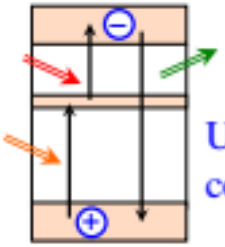 Up-conversion	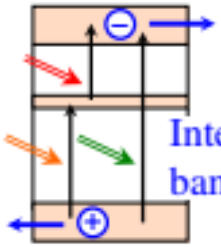 Intermediate-band	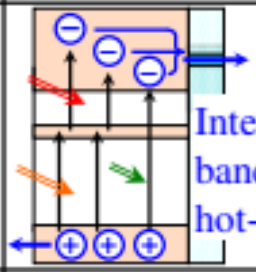 Intermediate-band-assisted hot-carrier
1 particle (high energy) ↓ 2 particles (low energy)	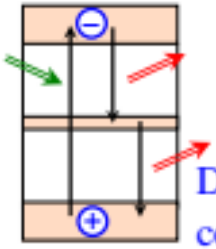 Down-conversion		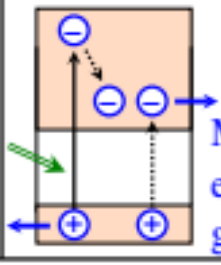 Multiple-exciton generation

Types of solar cells to exceed the Shockley–Quiseer limit.

Y. Takeda and T. Motohiro , Prog. Photovolt: Res. Appl. 2013; 21:1308–1318

Efficiency limits third generation solar cells

Limit	η (max. concentration) %	η (AM1.5) %
Lansberg	93.3	73.7
∞- cells	86.8	69.0
2 - cells	55.7	42.5
3 - cells	63.8	49.3
Hot carrier	85.0	65.0
IBSC	63.2	
MEG		
Down converter DC		36.7 (Si)
Up-converter		48 (Si)
Single junction Si	40.8	31.0

GREEN M.A., *Third generation photovoltaics: advanced solar electricity conversion*, Springer-Verlag, Berlin Heidelberg, 2006

Third generation solar cells
Very cheap, moderate efficincy (region 3b)
Emerging photovoltaics

Progress in perovskite solar cells

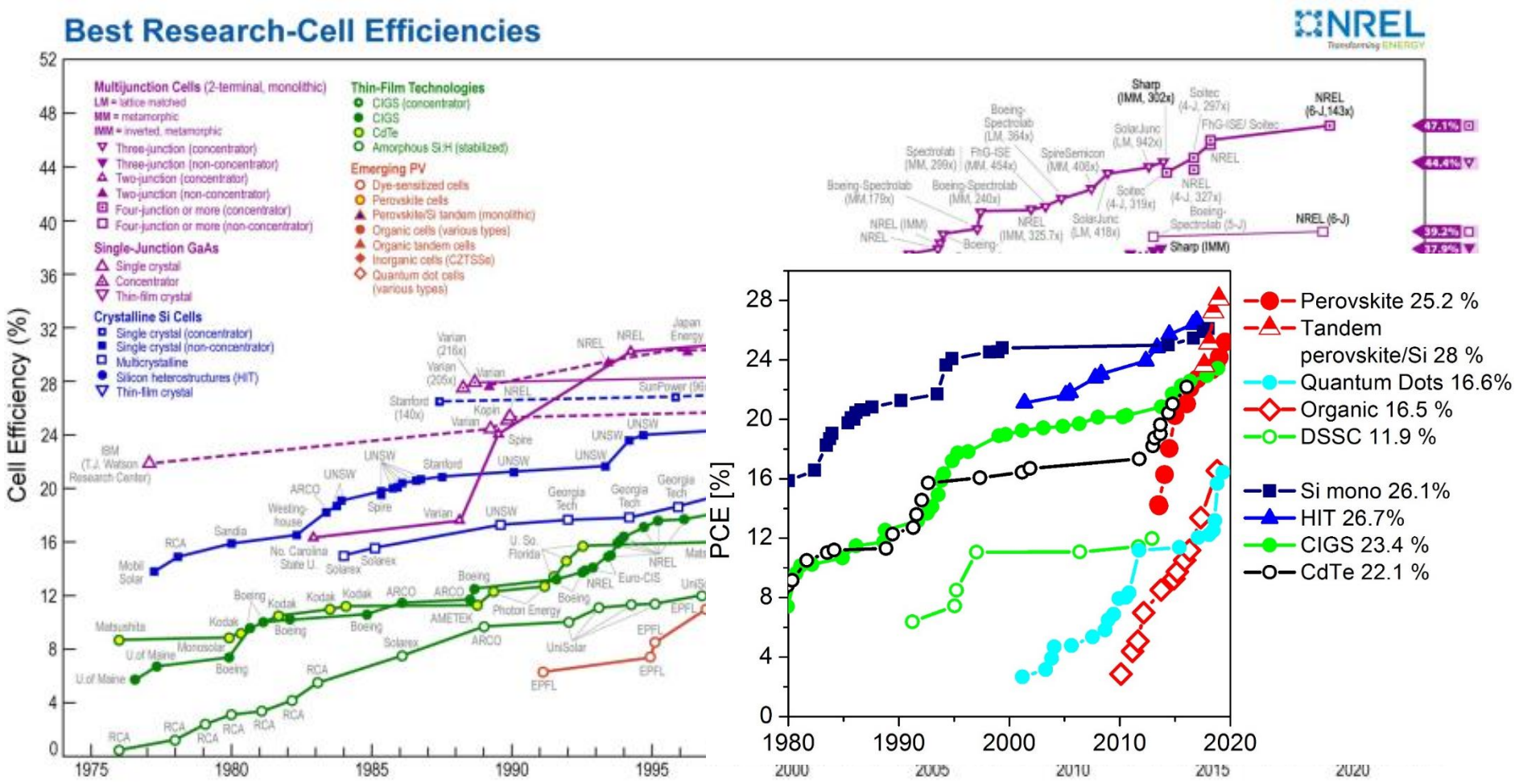

Theoretical PCE: Si 30 %

Tandem perovskite/Si 43%

HIT - *heterojunction with intrinsic thin-layer*

Rekordowe sprawności nowego typu ogniw („emerging PV”)

https://spectrum.ieee.org/static/interactive-record-breaking-pv-cells

	J_{sc} [mA/cm^2]	V_{oc} [mV]	FF [%]	PCE [%]	S [cm^2]	l. słońc	Instyt.	rok
DSSC	22,5	744	71,2	11,9	1,005	1	Sharp	09.2012
Perowskity	25,4	1170	79,8	**23,7**	0,074	1	ISCAS	09.2018
Perowskit/ Si tandem	19,76	1805	78,8	**28,0**	1,026	1	Oxford	12.2018
Organiczne	25,03	838	74,47	**15,6**	0,0411	1	CSU, SCUT	11.2018
Organiczne tandem	11,23	1610	73,3	13,2	0,041	1	eFlexPV, SCUT	09.2019
CZTSe	35,2	513	69,8	12,6	0,421	1	IBM	07.2013
Kropki kwantowe	18,1	1168	78,3	**16,6**	0,058	1	Univ. Qweensland	2018
Kropki kwantowe[1)]	14,3	950		13,4	0,0586	1	NREL	03.2017

(1) Abhishek Swarnkar, Ashley R. Marshall, Erin M. Sanehira, Boris D. Chernomordik, David T. Moore, Jeffrey A. Christians, Tamoghna Chakrabarti, Joseph M. Luther, *Quantum dot-induced phase stabilization of α-$CsPbI_3$ perovskite for high-efficiency photovoltaics*, Science, 354, 6308, p92, Oct. 7, 2016.

Thank you for your attention